

Research Note, submitted to the Canadian Journal of Remote Sensing

## Detection of coherent reflections with GPS bipath interferometry

Achim Helm, Georg Beyerle and Markus Nitschke  
GeoForschungsZentrum Potsdam, Dept. Geodesy & Remote Sensing, Potsdam,  
Germany

Corresponding author address: Achim Helm, GeoForschungsZentrum Potsdam, Dept. Geodesy  
& Remote Sensing, Telegrafenberg, D-14473 Potsdam, Germany. Tel.: +49-331-288-1812; fax:  
+49-331-288-1111. E-mail: helm@gfz-potsdam.de

**Abstract** Results from a GPS reflectometry experiment with a 12 channel ground-based GPS receiver above two lakes in the Bavarian Alps are presented. The receiver measures in open-loop mode the coarse/acquisition code correlation function of the direct and the reflected signal of one GPS satellite simultaneously. The interference between the coherently reflected signal and a model signal, which is phase-locked to the direct signal, causes variations in the amplitude of the in-phase and quad-phase components of the correlation sums. From these amplitude variations the relative altimetric height is determined within a precision of 2 cm.

## 1 Introduction

Satellite-based active altimeters on ENVISAT and JASON deliver valuable ocean height data sets for global climate modelling. In order to improve the climate models, altimetric data of higher resolution in space and time is required. This gap can potentially be filled with GPS-based altimetric measurements. Additionally, ground-based GPS receivers can monitor ocean heights in coastal areas where satellite altimetry data get coarse and decrease in quality (Fu and Cazenave, 2001; Shum et al., 1997).

Since GPS altimetry has been proposed as a novel remote sensing capability (Martín-Neira, 1993), many studies have been carried out at different observation heights and platforms. While Earth-reflected GPS signals have been observed from spaceborne instruments (Lowe et al., 2002a; Beyerle et al., 2002) and the CHAMP and SAC-C satellites already are equipped with Earth/nadir looking GPS antennas, work is in progress in order to establish satellite-based GPS altimetry (Hajj and Zuffada, 2003). Airborne campaigns have been conducted (e.g. Garrison et al. (1998), Garrison and Katzberg (2000), Rius et al. (2002)) and recently reached a 5-cm height precision (Lowe et al., 2002b). Ground-based GPS altimetry measurements have been performed at laboratory scale of some meters height with 1-cm height precision (Martín-Neira et al., 2002) up to low-altitudes height (e.g. Anderson (2000), Martín-Neira et al. (2001)) and reached a 2-cm height precision (Treuhaft et al., 2001).

In this study a 12 channel GPS receiver is used (Kelley et al., 2002), that has been extended with a coarse/acquisition (C/A) code correlation function tracking mode. In this coherent delay mapping (CDM) mode the direct GPS signal is tracked while concurrently the reflected signal is registered in open-loop mode. Using the L1 carrier phase the relative altimetric height is determined from the components of the reflected signal.

## 2 Experimental Setup and Data Acquisition

The experiment was conducted on 8 - 10 July 2003, 50 km south of Munich, Germany, in the Bavarian alpine upland at the mountain top of Fahrenberg (47.61°N, 11.32°E) at a height of about 1625 m asl. Mount Fahrenberg belongs to the Karwendel mountains and from the mountain top unobstructed view is available to lake Kochelsee (surface area about 6 km<sup>2</sup>) to the north and lake Walchensee (surface area about 16 km<sup>2</sup>) to the south. Following a schedule of predicted GPS reflection events, the receiver antenna was turned towards the lake surface of Kochelsee (about 599 m asl) or Walchensee (about 801 m asl). The antenna was tilted about 45° towards the horizon. During a GPS reflection event the direct and the reflected signals interfere at the antenna center (e.g. Parkinson and Spilker (1996)). The interference causes amplitude fluctuations that are quantitatively analyzed to determine the height variation of the specular reflection point.

The receiver is based on the OpenSource GPS design (Kelley et al., 2002) and was modified to allow for open-loop tracking of reflected signals. The receiving antenna is an active RHCP patch antenna (AT575-70C from AeroAntenna Technology Inc.) with 4 dBic gain, 54 mm in diameter and a hemispheric field-of-view. Operating in CDM mode all 12 correlator channels are tuned to the same GPS satellite by setting the appropriate pseudo-random noise (PRN) value. The correlation between the received and model (replica) signal is realized in hardware (Zarlink GP2021, ZARLINK (2001)). While one channel (the master channel) continues to track the direct signal, the carrier and code tracking loops of the 11 remaining channels (slave channels) are synchronized to the master channel. Each channel consists of the prompt and the early tracking arm at zero and at -0.5 chip code delay, respectively. Thus,  $2 \times 11 = 22$  delays are available to map the C/A code correlation function of the reflection signature. In CDM mode the slave carrier and code phase-locked loops (PLLs) are opened and their loop feed-back is obtained from the master PLL. All carrier loops operate with zero carrier phase offset with respect to the master channel; in the code loop feed-back, however, delays covering an interval of 2 chips (about 2  $\mu$ s) with a step size of 0.1 chips (about 100 ns) are inserted. In-phase and quad-phase correlation-sums of each channel are summed over 20 ms taking into account the navigation bit boundaries and stored together with code and carrier phases to hard disk at a rate of 50 Hz. Figure 2 illustrates the CDM mode: while the direct GPS signal is tracked with the prompt and early arm of the master channel at 0 and -0.5 chips code offset, the prompt and early arms of

the remaining 11 slave channels are set to chip code offsets between 0.4 and 2.7 to map the reflected signal (corresponding to an optical path difference of 120 to 810 m). In Figure 2 the root-sum-squared in-phase and quad-phase values of the reflected signal are plotted as a function of code delay. The maximum power of the reflected signal is about  $20 \log 0.2 = -14$  dB below the direct signal's power. The peak of the correlation function is separated by a delay of 1.5 chips from the direct signal's correlation peak.

Data analysis is performed in the following way: first, the code delay corresponding to the maximum of the reflected waveform is determined. Second, all in-phase and quad-phase correlation sum values  $I_r$  and  $Q_r$  are extracted from the raw data which lie within a certain delay interval (grey box in Figure 2) around the maximum code delay. The navigation message is demodulated according to

$$\begin{aligned}\tilde{I}_r &= \text{sign}(I_d) I_r \\ \tilde{Q}_r &= \text{sign}(I_d) Q_r,\end{aligned}\tag{1}$$

where  $I_d$  denotes the in-phase value of the master channel. Figure 3 A shows the oscillations of  $\tilde{I}_r$  and  $\tilde{Q}_r$  caused by the interference between the reflected and the replica GPS signal. The phasor  $\tilde{I}_r + i\tilde{Q}_r$  rotates by about  $+0.5$  Hz due to the decreasing path length difference between the direct and the reflected signal, since during this measurement the GPS satellite moved towards the horizon. Note the phase offset of  $90^\circ$  between  $\tilde{I}_r$  and  $\tilde{Q}_r$ . The phase  $\phi$  (Fig. 3 B) is calculated from the four quadrant arctangent

$$\phi = \text{atan2}(\tilde{Q}_r, \tilde{I}_r)\tag{2}$$

and is unwrapped by adding  $\pm 2\pi$  when the difference between consecutive values exceeds  $\pi$ , resulting in the accumulated phase  $\phi_a$ . The optical path length difference  $\delta$  between direct and reflected signal is calculated from the accumulated phase  $\phi_a$  and the L1 carrier wavelength  $\lambda_{L1} = 0.1903$  m at the observation time  $t$

$$\delta(t) = \frac{\phi_a(t)}{2\pi} \lambda_{L1}.\tag{3}$$

Starting with a height estimate  $H(t_0)$ , the temporal evolution of the altimetric height variation  $h(t) - h(t_0)$ , normal to the tangent plane at the reflection point P, is calculated from (Treuhaft et al., 2001)

$$h(t) = \frac{\delta(t) - \delta(t_0) + 2h(t_0) \sin \alpha(t_0)}{2 \sin \alpha(t)}\tag{4}$$

$$h(t_0) = (H(t_0) + r_E) \cos \frac{s}{r_E} - r_E\tag{5}$$

with the arclength  $s$  defined in Figure 1, an Earth radius  $r_E = 6371$  km and

$$\alpha = \epsilon + \frac{\pi}{2} - \gamma\tag{6}$$

$$\epsilon = \epsilon_{eph} + \Delta\epsilon_{tropo},\tag{7}$$

assuming an infinite distance to the GPS transmitter.  $\epsilon_{eph}$  is calculated from the broadcast ephemeris data (GPS SPS, 1995), the correction  $\Delta\epsilon_{tropo}$  accounts for refraction caused by atmospheric refractivity. The tropospheric correction is derived from a geometric raytracing calculation using a refractivity profile obtained from meteorological analyse provided by the European Centre for Medium-Range Weather Forecasts. The position of the specular reflection point P as function of  $\gamma$  (Figure 1) is calculated following Martín-Neira (1993).

Thus, the altimetric height change of the GPS receiver above the reflecting surface is determined from the carrier phase difference between the direct and reflected GPS signal (Figure 3 C).

### 3 Data Analysis and Discussion

During all 3 days several reflection events were observed from both lake surfaces with different GPS satellites at elevation angles between about  $10^\circ$  -  $15^\circ$ , indicated by a clearly visible waveform (see Figure 2). Several outliers can be observed in the data records. Most likely they are caused by overheating of the hardware correlator chip [S. Esterhuizen, University of Colorado, personal communication, 2003]. In this study outliers are removed in the following way: a value is calculated by linear extrapolation from the last 3 values of  $\tilde{I}_r(t)$ . If the difference between extrapolated and actual value exceeds a threshold (20000-22000), the extrapolated value is taken. The same is applied to the  $\tilde{Q}_r(t)$  data. Additionally cycle slips (sporadic height jumps of about  $\lambda_{L1}$  m in adjacent data points) can be observed in the optical path length difference  $\delta(t)$ . The distortion of the data by cycle slips could be minimized by applying the same method as above to  $\delta(t)$ . Continuous data segments without cycle slips are chosen for height change determination. The mean receiver height above the lake surface is not expected to change during the short analyzed time periods. From topographic maps (scale 1:25000, Bayerisches Landesvermessungsamt, 1987) the heights  $H(t_0)$  are estimated to be 1026 m  $\pm$  5 m (Kochelsee) and 824 m  $\pm$  5 m (Walchensee), respectively. By minimization of the linear trend of  $h(t) - h(t_0)$  we obtain a  $H(t_0)$  of 1022.5 m (Kochelsee) and 827.5 m (Walchensee).

Figure 4 A and B plot the relative height change between the receiver and the reflection point at the surface of lake Kochelsee. Both observations used the same PRN, but were taken on different days. The height varies within an interval of about  $\pm 5$  cm with a standard deviation of about 3.1 and 2.6 cm. Figure 4 C and D show the height changes between the receiver and the reflection point at the surface of lake Walchensee. Again both observations were taken on different days and used different PRNs. Compared to the Kochelsee data, the height varies within a height interval of about  $\pm 2.5$  cm with a standard deviation of about 1.4 and 1.7 cm.

The different height variations at both lakes can be explained by different local wind and wave height conditions. As lake Walchensee is completely surrounded by mountains, waves are mainly driven by local, thermal induced winds which mainly occur at noon. Lake Kochelsee is open to the north, so longer

lasting wind can build up waves on the lake surface.

## 4 Conclusions and Outlook

Open-loop tracking of the reflected signals allows the determination of the relative altimetric height with 2-cm precision. Different height changes can be observed at Kochelsee and Walchensee which reflect the different wind and wave height conditions at the two lakes. The relationship between the observed height changes and wind speed (e.g. Caparrini and Martin-Neira (1998), Lin et al. (1999), Komjathy et al. (2000), Zuffada et al. (2003), Cardellach et al. (2003)) will be subject of further studies. The present receiver implementation is limited to the observation of one GPS satellite at a time. To fully use the potential of GPS reflections the receiver will be modified to keep track of several GPS reflections simultaneously.

Our results suggest that open-loop tracking is possible with low-gain and wide field-of-view antennas, showing the potential of this method also for space-based measurements of GPS reflections.

## Acknowledgments

This work would not have been possible without the open source projects OpenSource GPS and RTAI-Linux. We thank Clifford Kelley and the developers of RTAI-Linux for making their work available. Helpful discussion with Robert Treuhaft and Philipp Hartl are gratefully acknowledged. We thank T. Schmidt, C. Selke and A. Lachmann for their help and technical support. The ECMWF provided meteorological analysis fields.

## References

- Anderson, K. (2000). Determination of water level and tides using interferometric observations of GPS signals. *Journal of Atmospheric and Oceanic Technology*, 17:1118–1127.
- Beyerle, G., Hocke, K., Wickert, J., Schmidt, T., and Reigber, C. (2002). GPS radio occultations with CHAMP: A radio holographic analysis of GPS signal propagation in the troposphere and surface reflections. *Journal of Geophysical Research*, 107(D24):doi:10.1029/2001JD001402.
- Caparrini, M. and Martin-Neira, M. (1998). Using reflected GNSS signals to estimate SWH over wide ocean areas. *ESTEC Working Paper*, 2003.
- Cardellach, E., Ruffini, G., Pino, D., Rius, A., Komjathy, A., and L., G. J. (2003). Mediterranean balloon experiment: ocean wind speed sensing from the stratosphere, using GPS reflections. *Remote Sensing of Environment*, 88(3):doi:10.1016/S0034-4257(03)00176-7.
- Fu, L. L. and Cazenave, A., editors (2001). *Satellite Altimetry and Earth Sciences*, volume 69 of *International Geophysical Series*. Academic Press.
- Garrison, J. L. and Katzberg, S. J. (2000). The application of reflected GPS signals to ocean remote sensing. *Remote Sensing of Environment*, 73:175–187.
- Garrison, J. L., Katzberg, S. J., and Hill, M. I. (1998). Effect of sea roughness on bistatically scattered range coded signals from the global positioning system. *Geophysical Research Letter*, 25(13):2257–2260.

- GPS SPS (1995). *GPS SPS Signal Specification*. GPS NAVSTAR, 2 edition.
- Hajj, G. and Zuffada, C. (2003). Theoretical description of a bistatic system for ocean altimetry using the GPS signal. *Radio Science*, 38(5):doi:10.1029/2002RS002787. 1089.
- Kelley, C., Barnes, J., and Cheng, J. (2002). OpenSource GPS: Open source software for learning about GPS. In *ION GPS 2002*, pages 2524–2533, Portland, USA.
- Komjathy, A., Zavorotny, V. U., Axelrad, P., Born, G. H., and Garrison, J. L. (2000). GPS signal scattering from sea surface: Wind speed retrieval using experimental data and theoretical model. *Remote Sensing of Environment*, 73:162–174.
- Lin, B., Katzberg, S. J., Garrison, J. L., and Wielicki, B. A. (1999). Relationship between GPS signals reflected from sea surfaces and surface winds: Modeling results and comparisons with aircraft measurements. *Journal of Geophysical Research*, 104(C9):20713 – 20727.
- Lowe, S. T., LaBrecque, J. L., Zuffada, C., Romans, L. J., Young, L. E., and Hajj, G. A. (2002a). First spaceborne observation of an earth-reflected GPS signal. *Radio Science*, 29(10):doi:10.1029/2000RS002539.
- Lowe, S. T., Zuffada, C., Chao, Y., Kroger, P., Young, L. E., and LaBrecque, J. L. (2002b). 5-cm-precision aircraft ocean altimetry using GPS reflections. *Geophysical Research Letter*, 29(10):doi:10.1029/2002GL014759.
- Martín-Neira, M. (1993). A passive reflectometry and interferometry system (PARIS): Application to ocean altimetry. *ESA Journal*, 17:331–355.
- Martín-Neira, M., Caparrini, M., Font-Rossello, J., Lannelongue, S., and Serra, C. (2001). The paris concept: An experimental demonstration of sea surface altimetry using GPS reflected signals. *IEEE Transactions on Geoscience and Remote Sensing*, 39:142–150.
- Martín-Neira, M., Colmenarejo, P., Ruffini, G., and Serra, C. (2002). Altimetry precision of 1 cm over a pond using the wide-lane carrier phase of gps reflected signals. *Canadian Journal of Remote Sensing*, 28(3):pp. 394–403.
- Parkinson, B., W. and Spilker, J. J., editors (1996). *Global Positioning System: Theory and Application*, volume 163 of *Progress in Astronautics and Aeronautics*. American Institute of Aeronautics and Astronautics.
- Rius, A., Aparicio, J. M., Cardellach, E., Martín-Neira, M., and Chapron, B. (2002). Sea surface state measured using GPS reflected signals. *Geophysical Research Letter*, 29(23):doi:10.1029/2002GL015524.
- Shum, C. K., Woodworth, P. L., Andersen, O. B., Egbert, G. D., Francis, O., King, C., Klosko, S. M., Le Provost, C., Li, X., Molines, J. M., Parke, M. E., Ray, R. D., Schlax, M. G., Stammer, D., Tierney, C. C., Vincent, P., and Wunsch, C. I. (1997). Accuracy assessment of recent ocean tide models. *Journal of Geophysical Research*, 102(C11):25173–25194.
- Treuhaft, R., Lowe, S., Zuffada, C., and Chao, Y. (2001). 2-cm GPS altimetry over Crater Lake. *Geophysical Research Letter*, 22(23):4343–4346.
- ZARLINK (2001). *GP2021 GPS 12 Channel Correlator*, DS4077-3.2 edition. <http://www.zarlink.com>.
- Zuffada, C., Fung, A., Parker, J., Okolicanyi, M., and Huang, E. (2003). Polarization properties of the gps signal scattered off a wind-driven ocean. *IEEE Transactions on Antennas and Propagation*.

## List of Symbols

$R$	receiver position
$P$	specular reflection point position
$\epsilon$	elevation angle of the GPS satellite above local horizon plane at R
$\delta$	observed path difference between direct and reflected signal path
$r_E$	Earth radius
$H$	receiver height
$h$	height variations normal to tangential plane at P
$\alpha$	angle of reflection above tangential plane at P
$\gamma$	angle between normal of tangential plane and local horizon plane at P
$s$	arc length from subreceiver point to specular reflection point P
$I_d$	in-phase correlation sum of the direct data
$I_r$	in-phase correlation sum of the reflected data
$Q_r$	quad-phase correlation sum of the reflected data
$\tilde{I}_r$	$I_r$ demodulated from navigation message
$\tilde{Q}_r$	$Q_r$ demodulated from navigation message
$\phi$	phase
$\phi_a$	accumulated phase
$\lambda_{L1}$	L1 carrier wavelength
$\epsilon_{eph}$	elevation angle calculated from broadcast ephemeris data
$\Delta\epsilon_{tropo}$	tropospheric correction to elevation angle

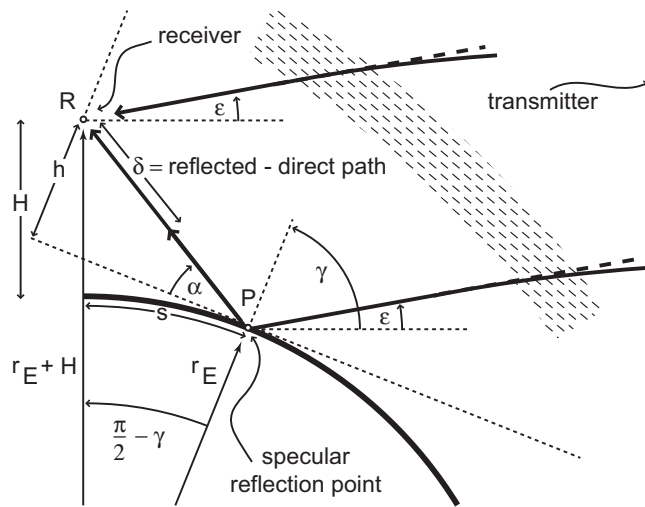


Figure 1: Geometry used to express the observed path difference  $\delta$  in terms of the known receiver position R with height H and the GPS satellite elevation angle  $\epsilon$  and the calculated position of the specular reflection point P.  $h$  denotes the height variations normal to the tangential plane at P. Note that  $\epsilon$  has to be corrected by  $\Delta\epsilon_{tropo}$  due to the bending effect caused by the Earth's troposphere.



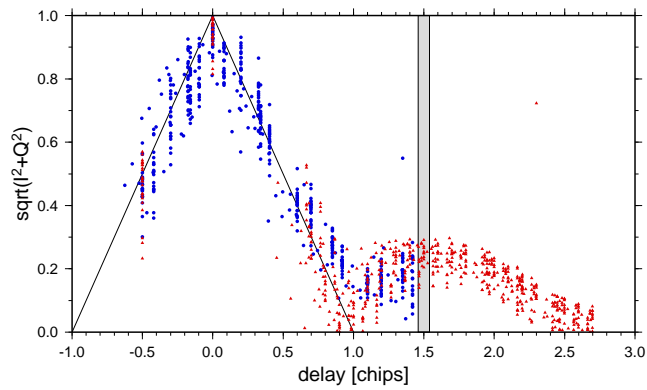


Figure 2: Delay mapped waveform of a reflection event (PRN 16) at 1334:17 UTC 8 July 2003, antenna oriented towards Kochelsee. The delay is given in relation to the maximum peak of the direct signal. Blue circles and red triangles indicate 2 measurements (0.5-second duration) starting 120 (blue) and 267 (red) seconds after the start of the measurement. In the second case (red) the 2-chip-wide interval of covered chip code offsets is centered at the maximum of the reflected signal. The points reveal the measured waveform of the direct and reflected correlation signal. The thin black triangle marks the theoretical C/A code correlation function of the direct signal. The grey box marks the maximum of the reflected signal.

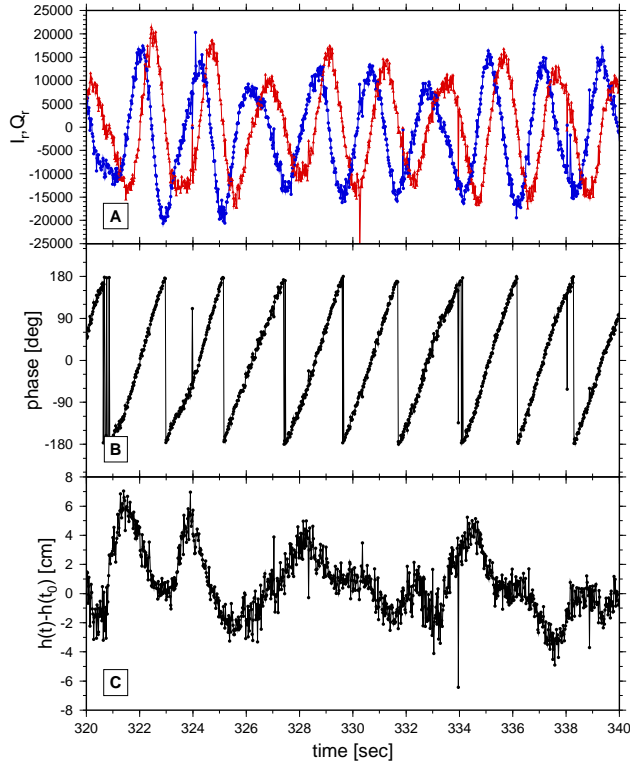


Figure 3: Panel A shows the demodulated reflected in- and quad-phase data  $\tilde{I}_r$  (blue circles) and  $\tilde{Q}_r$  (red triangles) (PRN 16, elevation from  $11.04^\circ$  to  $10.99^\circ$ ), antenna oriented towards Kochelsee at 1334:17 UTC 8 July 2003, as a function of time since measurement start. With Eq. 2 the phase  $\phi$  (Panel B) and from Eq. 4 and 5 the relative height  $h(t) - h(t_0)$  is calculated (Panel C), with  $H(t_0) = 1022.5$  m.

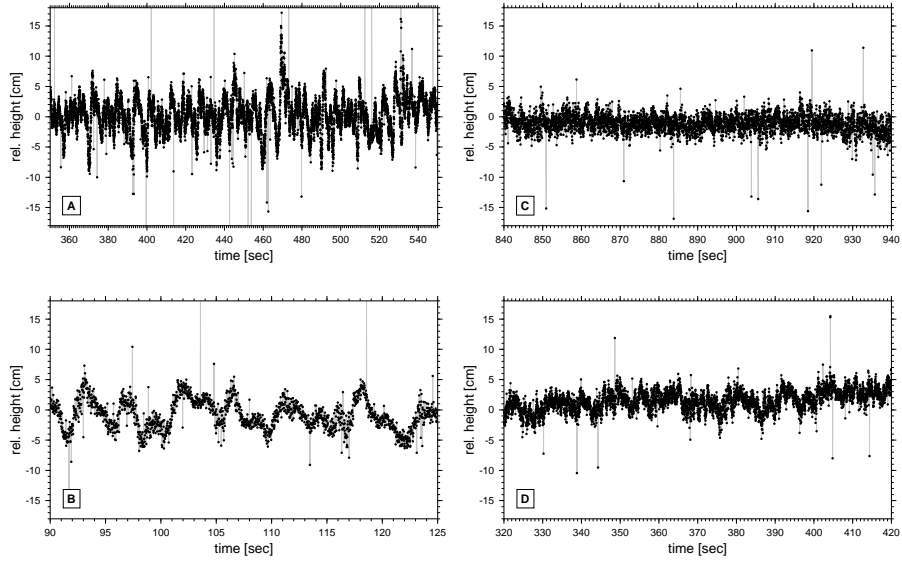


Figure 4: The left panels show relative height measurements at Kochelsee (PRN 16), starting at 1334:17 UTC 8 July 2003 (Panel A) and starting at 1327:17 UTC 10 July 2003 (Panel B) as a function of time since the start of the observation. PRN 16 changed elevation from  $11.0^\circ$  to  $10.4^\circ$  (Panel A) and from  $11.4^\circ$  to  $11.3^\circ$  (Panel B). On the right panels height measurements at Walchensee are shown, PRN 20 (elevation from  $14.7^\circ$  to  $14.1^\circ$ ), starting at 1257:15 UTC 8 July 2003 (Panel C) and PRN 11 (elevation from  $14.3^\circ$  to  $13.6^\circ$ ), starting at 1110:21 UT 9 July 2003 (Panel D).  $H(t_0) = 1022.5$  m (Kochelsee) and  $H(t_0) = 827.5$  m (Walchensee).